Published in final edited form as:
Inflamm Bowel Dis. 2009 May ; 15(5): 697–706. doi:10.1002/ibd.20827.

GlcNAc6ST-1-Mediated Decoration of MAdCAM-1 Protein with L-Selectin Ligand Carbohydrates Directs Disease Activity of Ulcerative Colitis

Motohiro Kobayashi, MD, PhD[*], **Hitomi Hoshino, MS**[*], **Junya Masumoto, MD, PhD**[*], **Mana Fukushima, MD**[†], **Kenichi Suzawa, MD, PhD**[*,‡], **Shunsuke Kageyama, MS**[*], **Manabu Suzuki, PhD**[*], **Haruo Ohtani, MD, PhD**[§], **Minoru Fukuda, PhD**[|], and **Jun Nakayama, MD, PhD**[*]

[*] Department of Molecular Pathology, Shinshu University Graduate School of Medicine, Matsumoto, Japan

[†] Department of Laboratory Medicine, Shinshu University Hospital, Matsumoto, Japan

[‡] Department of Internal Medicine, Shinshu University Hospital, Matsumoto, Japan

[§] Department of Pathology, Mito Medical Center, National Hospital Organization, Ibaraki, Japan

[|] Tumor Microenvironment Program, Cancer Research Center, Burnham Institute for Medical Research, La Jolla, California

Abstract

Background—A diffuse lymphocyte infiltrate is one of the characteristic features of ulcerative colitis (UC). Such lymphocyte recruitment requires lymphocyte rolling mediated by L-selectin ligand carbohydrates (6-sulfo sialyl Lewis X-capped *O*-glycans) and/or mucosal addressin cell adhesion molecule 1 (MAdCAM-1) expressed on high endothelial venule (HEV)-like vessels. The present study was undertaken to elucidate the role of MAdCAM-1 posttranslationally modified ("decorated") with L-selectin ligand carbohydrates in UC pathogenesis and consequent clinical outcomes.

Methods—Biopsy specimens composed of active and remission phases of UC as well as normal colonic mucosa were immunostained for CD34, MAdCAM-1 and MECA-79, and the immunostained sections were quantitatively analyzed. RT-PCR was carried out to evaluate transcripts of MAdCAM-1 and *N*-acetylglucosamine-6-*O*-sulfotransferases (GlcNAc6STs). CHO and Lec2 cells transfected with CD34 and MAdCAM-1 together with enzymes involved in L-selectin ligand carbohydrate biosynthesis were analyzed by immunofluorescence, FACS and Western blotting to characterize biochemical property of GlcNAc6STs.

Results—The number of MAdCAM-1$^+$ vessels was increased in UC, with no significant difference between active and remission phases. An increased ratio of MECA-79$^+$ to MAdCAM-1$^+$ vessels with preferential GlcNAc6ST-1 transcripts was observed in the active phase of UC compared to remission phase. MAdCAM-1 protein was co-localized with L-selectin ligand carbohydrates at the luminal surface of HEV-like vessels *in situ*. GlcNAc6ST-1 preferentially utilizes MAdCAM-1 as a scaffold protein for GlcNAc-6-*O*-sulfation in L-selectin ligand carbohydrate biosynthesis.

Correspondence and Reprints: Motohiro Kobayashi, MD, PhD, Department of Molecular Pathology, Shinshu University Graduate School of Medicine, 3-1-1 Asahi, Matsumoto 390-8621, Japan (e-mail: motokoba@shinshu-u.ac.jp). Phone: +81-263-37-3395, FAX: +81-263-37-2581.

Conclusions—UC disease activity is not regulated by expression of MAdCAM-1 protein itself, but rather by GlcNAc6ST-1-mediated decoration of MAdCAM-1 protein with L-selectin ligand carbohydrates.

Keywords

ulcerative colitis; mucosal addressin cell adhesion molecule 1 (MAdCAM-1); peripheral lymph node addressin (PNAd); L-selectin ligand carbohydrate; posttranslational modification

INTRODUCTION

Ulcerative colitis (UC) is a chronic, relapsing inflammatory disorder affecting the colonic mucosa. Although its etiopathogenesis remains unclear, it is currently considered an abnormal inflammatory response to intestinal microbial flora with or without components of autoimmunity (1). In UC, in addition to cryptitis/crypt abscess, a diffuse chronic inflammatory cell infiltrate composed mainly of lymphocytes and plasma cells in the lamina propria is almost universally present (2). It is widely accepted that these inflammatory cells use extravasation mechanisms operating in normal conditions, although in an uncontrolled manner (3).

Lymphocyte homing and lymphocyte recruitment during chronic inflammation are mediated by a cascade of adhesive interactions between circulating lymphocytes and specialized endothelial cells comprising high endothelial venules (HEVs) (4,5). At least one of the two molecular interactions is required for the initial step of tethering and rolling—one via L-selectin and peripheral lymph node addressin (PNAd) (6) and the other viaα4β7 integrin and mucosal addressin cell adhesion molecule 1 (MAdCAM-1) (7). These interactions trigger lymphocyte chemokine-dependent activation, integrin-mediated firm attachment to the endothelium, and transmigration across blood vessels (4,5).

PNAd, a glycoprotein complex recognized by the MECA-79 monoclonal antibody (8), is constitutively displayed on HEVs of secondary lymphoid organs, namely peripheral lymph nodes and tonsils, and functions in L-selectin-dependent lymphocyte homing (9). The MECA-79 epitope has been shown to be 6-sulfo *N*-acetyllactosamine attached to extended core 1 *O*-glycans, Galβ1→4(SO_3^-→6)GlcNAcβ1→3Galβ1→3GalNAcα1→Ser/Thr 4(SO_3 (Fig. 1) (10). The MECA-79 antibody also reacts with its sialylated and fucosylated form, 6-sulfo sialyl Lewis X attached to extended core 1 *O*-glycans, sialic acidα2→3Galβ1→4[Fucα1→3(SO_3^-→6)]GlcNAcβ1→3Galβ1→3GalNAcα1→Ser/Thr (Fig. 3(SO_3 1) (10). Although absent under normal conditions, in chronic inflammatory states PNAd is induced on HEV-like vessels (9,11–13). In this context, we previously showed preferential induction of PNAd-expressing HEV-like vessels in the active phase of UC and close association of T cells, particularly $CD4^+$ T cells, with these vessels, suggesting that T cell recruitment via PNAd-expressing HEV-like vessels functions in UC pathogenesis (14).

MAdCAM-1 is an endothelial adhesion molecule belonging to the immunoglobulin superfamily and is constitutively displayed on HEVs in Peyer's patches and mesenteric lymph nodes and on flattened venular endothelial cells in the intestinal lamina propria (15). MAdCAM-1 functions in control of α4β7 integrin-expressing memory/effector lymphocyte homing (4,9,16,17). Similar to other members of integrin family, α4β7 integrin requires chemokine-dependent activation for firm attachment to MAdCAM-1 (4,7,17); however, without activation, it can weakly bind to MAdCAM-1, contributing to L-selectin-independent tethering and rolling of α4β7 integrin-expressing memory/effector lymphocytes in mucosal lymphocyte homing (16,17). In addition to its function as an α4β7 integrin

receptor, MAdCAM-1 can be posttranslationally modified ("decorated") with L-selectin ligand carbohydrates at its mucin-like domain and supports L-selectin-dependent lymphocyte rolling (18). MAdCAM-1 is thus a dual-function molecule capable of serving as a vascular addressin for both L-selectin and α4β7 integrin, which may cooperate and potentially synergize in mucosal lymphocyte homing (18). Several reports showed increased MAdCAM-1 expression at inflamed sites of UC, suggesting that α4β7 integrin/MAdCAM-1 interactions may in part mediate lymphocyte recruitment in UC (15,19,20); however, the consequence of MAdCAM-1 decoration with L-selectin ligand carbohydrates remains to be clarified.

Sulfation of L-selectin ligand carbohydrates is a prerequisite for functional L-selectin binding activity (21,22). To date, five *N*-acetylglucosamine-6-*O*-sulfotransferases (GlcNAc6STs) have been identified in humans (23). Among them, GlcNAc6ST-1 (24) and GlcNAc6ST-2 (22) are implicated in GlcNAc-6-*O*-sulfation to form 6-sulfo sialyl Lewis X-capped *O*-glycans (Fig. 1) on HEVs (9). Between the two enzymes, HEV-restricted GlcNAc6ST-2 plays a dominant role in PNAd biosynthesis; however, GlcNAc6ST-1 is suggested to be the primary intestinal GlcNAc6ST, particularly in Peyer's patches, since MECA-79 staining of Peyer's patches is abrogated in mice lacking GlcNAc6ST-1 (25). Consistent with this, GlcNAc6ST-1 is suggested to regulate sulfation of PNAd on HEV-like vessels induced in UC, because GlcNAc6ST-1 transcripts are detected almost exclusively in the active but not remission phase of UC (14). Given that MAdCAM-1 is not expressed in peripheral lymph nodes but expressed predominantly in small and large intestine and associated lymphoid tissue such as mesenteric lymph nodes (15,26), sulfation of L-selectin ligand carbohydrates on MAdCAM-1 is likely mediated by GlcNAc6ST-1.

Here we show increased numbers of MAdCAM-1^+ vessels in UC but found no significant difference between active and remission phases. We also observed an increased ratio of MECA-79^+ to MAdCAM-1^+ vessels with increased transcripts of GlcNAc6ST-1 in the active phase of UC compared to remission phase. Moreover, we show that GlcNAc6ST-1 preferentially utilizes MAdCAM-1 as a scaffold protein for GlcNAc-6-*O*-sulfation in L-selectin ligand carbohydrate biosynthesis. Given co-localization of L-selectin ligand carbohydrates with MAdCAM-1 protein at the luminal surface of HEV-like vessels *in situ*, these results overall suggest that UC disease activity is not regulated by expression of MAdCAM-1 protein itself but rather by GlcNAc6ST-1-mediated decoration of MAdCAM-1 protein with L-selectin ligand carbohydrates.

MATERIALS AND METHODS

Histological Samples

The analysis of human tissues was approved by the Ethical Committee of Shinshu University School of Medicine. Formalin-fixed, paraffin-embedded (FFPE) blocks of biopsied specimens with established UC diagnosis were retrieved from the archives of the Department of Laboratory Medicine, Shinshu University Hospital, and divided into active (N = 32) and remission (N = 12) phase groups, based on the UC Disease Activity Index (UCDAI) as described (14,27,28). Biopsy specimens without inflammatory and cancerous lesions (N = 10) served as controls.

Immunohistochemistry

Monoclonal antibodies serving as primary antibodies were: QBEND10 (directed to human CD34, mouse IgG) (Immunotech, Luminy, France), 1C3 (directed to human MAdCAM-1, mouse IgG) (20), and MECA-79 (recognizing 6-sulfo *N*-acetyllactosamine attached to

extended core 1 *O*-glycans, which constitute PNAd, rat IgM) (BD Pharmingen, San Diego, CA) (8).

Tissue sections were immunostained by the labeled streptavidin-biotin (LSAB) method as described (14). Briefly, after quenching endogenous peroxidase activity with 0.3% H_2O_2 methanol solution, sections were blocked with 1% bovine serum albumin (BSA) (Sigma-Aldrich, St. Louis, MO) in phosphate-buffered saline (PBS). After incubation with primary antibody, sections were incubated with host- and class-matched biotinylated secondary antibody (Dako, Kyoto, Japan), followed by incubation with horseradish peroxidase (HRP)-conjugated streptavidin (Dako). The color reaction was developed with 3,3′-diaminobenzidine (DAB) (Dojindo, Kumamoto, Japan) containing 0.02% H_2O_2. Sections were briefly counterstained with hematoxylin. Negative controls were obtained by replacing primary antibodies with isotype-matched immunoglobulins, which showed no specific stainings.

For 44 UC and 10 normal colon samples, the number of $CD34^+$, MAdCAM-1^+, and MECA-79^+ lamina propria vessels in five high power fields of view using x400 magnification was counted using a BX51 light microscope (Olympus, Tokyo, Japan). MAdCAM-1^+/$CD34^+$ and MECA-79^+/MAdCAM-1^+ vessel ratios were calculated as described without knowledge of clinical status (14).

Double Immunofluorescence Staining

For double immunofluorescence staining for MAdCAM-1 and PNAd, sections were incubated with 1C3 followed by incubation with rhodamine-conjugated goat $F(ab')_2$ fragment of anti-mouse IgG (H+L) (Immunotech). Sections were then incubated with MECA-79 antibody and then with fluorescein isothiocyanate (FITC)-conjugated goat $F(ab')_2$ fragment of anti-rat IgM (Immunotech). Sections were mounted with Vectashield (Vector, Burlingame, CA) and viewed under an AX-80 fluorescence microscope (Olympus) and a laser confocal microscope LSM510 (Carl Zeiss, Jena, Germany).

Reverse Transcription Polymerase Chain Reaction

Total RNA was extracted from FFPE tissue sections, and single-stranded cDNA was synthesized as described (14). Polymerase chain reaction (PCR) was then carried out as described (14) with primers for MAdCAM-1, 5′-ACGCAGGGAGAAGTGATCCCAACA-3′ (5′-primer) and 5′-TTTCCAGAGGTGATACGTGGGCAA-3′ (3′-primer); GlcNAc6ST-1, 5′-TCCTCCAAGCCTTTCGTGGTATCT-3′ (5′-primer) and 5′-TGGTAGCAAAACTCCTCCACCTGT-3′ (3′-primer); GlcNAc6ST-2, 5′-TTCTGCACCTGCCTGTGACATCAT-3′ (5′-primer) and 5′-GTAGAGGGACTGCAGGTTGAAGAA-3′ (3′-primer); and glyceraldehyde-6-phosphate dehydrogenase (GAPDH), 5′-TGAGTACGTCGTGGAGTCCACT-3′ (5′-primer) and 5′-CAGAGATGATGACCCTTTTGGCTC-3′ (3′-primer). After initial denaturation at 94°C for 2 min, PCR conditions were: denaturation at 96°C for 20 sec, annealing at 60°C for 30 sec, extension at 72°C for 30 sec, and a final extension at 72°C for 2 min. The number of amplifications was 40 for GlcNAc6ST-1 and MAdCAM-1, 35 for GAPDH, and 30 for GlcNAc6ST-2. In the case of GlcNAc6ST-2, 1 μl of the above PCR reaction diluted 1:1,000 was subjected to nested PCR substituting the 3′-primer with 5′-CACCACCTCAAAGGGCTGTTGACT-3′ under the same condition. Negative (minus template) and positive (1 pg of plasmid DNA harboring target cDNA) control amplifications were performed in every experiment. PCR products were electrophoresed on 2% agarose gels containing 0.1 μg/ml of ethidium bromide and visualized under ultraviolet light.

Cloning of cDNA Encoding Human MAdCAM-1 and GlcNAc6ST-1

cDNAs encoding human MAdCAM-1 and GlcNAc6ST-1 were cloned by PCR using PrimeSTAR® Max DNA Polymerase (TaKaRa, Kyoto, Japan). In the case of GlcNAc6ST-1, cDNA starting from the most possible initiation methionine, that is 47 amino acids upstream from the previously reported methionine (24), was cloned since it was judged by the results of PSORT II, a program to predict the subcellular localization sites of proteins from their amino acid sequence (http://psort.ims.u-tokyo.ac.jp/) (29), that the longer form of GlcNAc6ST-1 has a better association with the membrane (endoplasmic reticulum (ER) 17.4% and Golgi 13.0% for the longer form vs. ER 8.7% and Golgi 4.3% for the shorter form). Primers were as follows: MAdCAM-1, 5′-GCAAGCTTGACTGAGCATGGATTTCGGACTG-3′ (5′-primer) and 5′-ATGAATTCTCAGGAGGGGCTGATCCCGAC-3′ (3′-primer) (HindIII and EcoRI sites underlined); GlcNAc6ST-1, 5′-TCGAATTCTGTGCCTGTGATGAGCCGCAGC-3′ (5′-primer) and 5′-AGCTCGAGTTAGAGACGGGGCTTCCGAAGCA-3′ (3′-primer) (EcoRI and XhoI sites underlined). cDNA from human small intestine (Clontech, Mountain View, CA) was used as template. The 3′-ends of amplified DNA fragments were first tailed with dATP using Ex Taq® DNA polymerase (TaKaRa), and inserted into pCR2.1-TOPO (Invitrogen, Carlsbad, CA). cDNAs encoding MAdCAM-1 and GlcNAc6ST-1 in pCR2.1-TOPO were digested with HindIII and EcoRI, and EcoRI and XhoI, respectively, and subcloned into the HindIII-EcoRI and EcoRI-XhoI sites, respectively, of pcDNA1, resulting in pcDNA1-MAdCAM-1 and pcDNA1-GlcNAc6ST-1. pcDNA1-CD34 and pcDNA1-GlcNAc6ST-2 were cloned previously (22).

To express soluble human CD34 and MAdCAM-1, cDNAs encoding amino acid residues 1–288 of CD34 and 1–342 of MAdCAM-1 were similarly amplified by PCR, and inserted into pCR2.1-TOPO. Primers were as follows: CD34, 5′-GGGGTACCGCGGGAAGGATGCTGGTCCGCAG-3′ (5′-primer) and 5′-GAAGATCTTGGGAATAGCTCTGGTGGCTTGC-3′ (3′-primer) (KpnI and BglII sites underlined); MAdCAM-1, 5′-GGGGTACCGACTGAGCATGGATTTCGGACTGG-3′ (5′-primer) and 5′-CGGGATCCAGCTGGTCACCCGCAGGTTTGGA-3′ (3′-primer) (KpnI and BamHI sites underlined). Partial cDNAs for CD34 and MAdCAM-1 in pCR2.1-TOPO were digested with KpnI and BglII, and KpnI and BamHI, respectively, and subcloned into the KpnI-BamHI sites of pcDNA3-IgG, which harbors the human IgG hinge plus constant region (30), resulting in pcDNA3-CD34•IgG and pcDNA3-MAdCAM-1•IgG, respectively.

Expression of MECA-79 Epitope on CD34 and MAdCAM-1 on Lec2 Cells

Lec2 cells (31) were transiently transfected with pcDNA1-CD34, pcDNA1-MAdCAM-1, or pcDNA1 (mock) combined with pcDNA3-core 1 extendingβ1,3-*N*-acetylglucosaminyltransferase (Core1-β3GlcNAcT) (10) and either pcDNA1-GlcNAc6ST-1, pcDNA1-GlcNAc6ST-2, or pcDNA1 (mock) using Lipofectamine Plus (Invitrogen) as manufacturer's instruction. CHO mutant Lec2 cells were used, since this line lacks Golgi-sialylation (31), and thus core 1 extension does not compete withα2,3-sialylation of core 1 *O*-glycans (Galβ1→3GalNAcα1→Ser/Thr) (see Fig. 1). Thirtysix hours later, transfected cells were doubly immunostained with MECA-79 and QBEND10 and/or 1C3 as described above and viewed under an AX-80 fluorescence microscope. To express soluble proteins, pcDNA1-CD34•IgG and pcDNA1-MAdCAM-1•IgG, respectively, were substituted for pcDNA1-CD34 and pcDNA1-MAdCAM-1.

Establishment of CHO Cells Stably Expressing MAdCAM-1 Decorated with Non-Sulfated Sialyl Lewis X Attached to Extended Core 1 *O*-Glycans

CHO cells were stably co-transfected with pcDNA1-MAdCAM-1 and pcDNA3.1 (Invitrogen) and selected in 400 μg/ml of Geneticin (Sigma-Aldrich). 1C3-positive cells

were cloned by limited dilution resulting in CHO-MAdCAM-1. Cells were then stably co-transfected with pCDM8-α1,3-fucosyltransferase VII (FucT-VII) (32) and pcDNA3.1/Zeo (Invitrogen) and selected in Geneticin and 100 μg/ml of Zeocin (Invitrogen). Cells positive for HECA-452, which recognizes sialyl Lewis X in both *O*- and *N*-glycans (13,33), were cloned, resulting in CHO-MAdCAM-1/FucT-VII. Cells were further stably co-transfected with pcDNA3-Core1-β3GlcNAcT and pcDNA3.1/Hyg (Invitrogen) and selected in Geneticin, Zeocin, and 400 μg/ml of Hygromycin B (Invitrogen). After transient transfection with pcDNA1-GlcNAc6ST-2, MECA-79-positive cells were cloned, resulting in CHO-MAdCAM-1/FucT-VII/Core1-β3GlcNAcT. CHO-CD34/FucT-VII/Core1-β3GlcNAcT has been established previously (22).

The resultant CHO-MAdCAM-1/FucT-VII/Core1-β3GlcNAcT and CHO-CD34/FucT-VII/Core1-β3GlcNAcT lines were then transiently transfected with either pcDNA1-GlcNAc6ST-1, pcDNA1-GlcNAc6ST-2, or pcDNA1 (mock), dissociated thirtysix hours later into monodispersed cells using Hanks'-based enzyme-free Cell Dissociation Buffer (Invitrogen), and stained with MECA-79 and either QBEND10 or 1C3 as described above. Stained cells were subjected to FACS analysis using a FACSort (BD Biosciences, San Jose, CA) with CellQuest Pro software (BD Biosciences).

Western Blotting Analysis

CD34•IgG and MAdCAM-1•IgG in the culture medium of Lec2 cells were purified by Protein A-Sepharose® (Sigma-Aldrich), lysed in sample buffer, and incubated at 65°C for 15 min. Each sample was separated by 10% sodium dodecyl sulfate-polyacrylamide gel electrophoresis (SDS-PAGE) and transferred onto a polyvinylidene difluoride (PVDF) membrane (Millipore, Billerica, MA). After blocking in Tris-bufferd saline (TBS) containing 5% (w/v) nonfat dry milk for 60 min, the membrane was incubated with QBEND10, 1C3, or MECA-79, followed by HRP-conjugated $F(ab')_2$ fragment of anti-mouse IgG or anti-rat IgM (Jackson Immunoresearch, West Grove, PA). The membrane was developed using the ECL system (Amersham Pharmacia Biotech, Piscataway, NJ).

Statistical Analysis

All data are expressed as means ± SEM. Differences between groups were statistically analyzed by the Kruskal-Wallis test, followed by Dunn's post-test for pairwise comparisons, using InStat 3 software (GraphPad Software, San Diego, CA). *P* values less than 0.05 were considered significant.

RESULTS

Increased Frequency of MAdCAM-1$^+$ Vessels in UC

To quantitate changes in MAdCAM-1 expression associated with UC we performed immunohistochemistry for CD34, MAdCAM-1, and PNAd and evaluated proportions of MAdCAM-1$^+$ vessels among CD34$^+$ vessels in colonic mucosa with UC in active and remission phases as well as in normal colonic mucosa. In normal mucosa, MAdCAM-1 was expressed sporadically on the luminal surface of venular endothelial cells in lamina propria (data not shown), while MAdCAM-1$^+$ vessels were frequently observed in colonic mucosa with UC, regardless of UC disease activity (Fig. 2). The percentage of MAdCAM-1$^+$ vessels in both active (9.23%) and remission (8.53%) UC phases was greater than that seen in normal colonic mucosa (0.885%), with high statistical significance ($P < 0.001$ and $P < 0.01$, respectively), while differences between the two UC phases did not differ significantly (Fig. 3, left). This finding suggests that the number of MAdCAM-1$^+$ vessels increases with active UC onset, but does not decrease significantly with clinical remission.

Increased Ratio of MECA-79$^+$ to MAdCAM-1$^+$ Vessels in the Active Phase of UC

We next evaluated the percentage of MECA-79$^+$ vessels among MAdCAM-1$^+$ vessels. MECA-79$^+$ vessels were not detected in normal colonic mucosa, while they were frequently observed in UC, particularly in the active phase (Fig. 2). The percentage of MECA-79$^+$ vessels among MAdCAM-1$^+$ vessels in active phase (66.5%) was greater than that seen in remission phase (7.62%), with high statistical significance ($P < 0.01$) (Fig. 3, right). These results overall indicate that the number of MECA-79$^+$ vessels, but not MAdCAM-1$^+$ vessels, increases in the active phase of UC compared to remission phase, suggesting that UC disease activity is not facilitated by expression of MAdCAM-1 protein, but instead by L-selectin ligand carbohydrates displayed on that protein.

Co-Localization of L-Selectin Ligand Carbohydrates with MAdCAM-1 Protein *In Situ*

To confirm co-localization of L-selectin ligand carbohydrates with MAdCAM-1 protein *in situ*, we carried out double immunofluorescence staining on FFPE tissue sections with active UC. As shown in Fig. 4, MAdCAM-1 protein was expressed on almost the entire circumference of high endothelial cells predominantly at the luminal surface (Fig. 4A, D, and G). On the other hand, L-selectin ligand carbohydrates, as detected by MECA-79 staining, were expressed on the luminal surface of those endothelial cells (Fig. 4B, E, and H). Co-localization of L-selectin ligand carbohydrates with MAdCAM-1 protein was confirmed mostly at the luminal surface of HEV-like vessels (Fig. 4C, F, and I). This finding indicates that, while MAdCAM-1 protein is expressed on the entire circumference of high endothelial cells, glycosylation and sulfation to form L-selectin ligand carbohydrates takes place preferentially at the luminal surface of those cells.

Preferential Expression of the Gene Encoding GlcNAc6ST-1 in the Active Phase of UC

To determine the identity of the GlcNAc6ST protein largely responsible for PNAd biosynthesis in colonic mucosa with UC, we carried out RT-PCR. As shown in Fig. 5, GlcNAc6ST-1 transcripts were detected in all samples of active phase UC and in normal colonic mucosa, but in three of five samples with UC in remission phase. On the other hand, even after confirmation using nested PCR, GlcNAc6ST-2 transcripts were detected in only one of five samples with UC in active phase and two of five normal colonic mucosa samples. As shown previously (14) and confirmed here, GlcNAc6ST-2 transcripts were not detected in any sample with UC in remission phase. These results suggest that GlcNAc6ST-1 is likely a key sulfotransferase controlling GlcNAc-6-*O*-sulfation in PNAd biosynthesis on HEV-like vessels induced in UC. Additionally, MAdCAM-1 transcripts were detected in most UC samples, regardless of disease activity, as well as in normal colonic mucosa, a finding consistent with the above immunohistochemical results.

Scaffold Protein-Dependent Sulfation by GlcNAc6ST-1

To determine which GlcNAc6ST functions in GlcNAc-6-*O*-sulfation to form the MECA-79 epitope on MAdCAM-1, Lec2 cells were transiently transfected with either CD34 or MAdCAM-1 cDNA, to create a scaffold protein and then with Core1-β3GlcNAcT and either GlcNA6ST-1, GlcNAc6ST-2 cDNAs, or pcDNA1 (mock). As shown in Fig. 6, GlcNAc6ST-2 transferred sulfate to form the MECA-79 epitope on both exogenous scaffold proteins and on endogenous Lec2 cell membrane proteins. Intriguingly, GlcNAc6ST-1, on the other hand, transferred sulfate to form the MECA-79 epitope on MAdCAM-1, but such sulfation was not detected on CD34 or on endogenous Lec2 cell proteins. Taken together, GlcNAc6ST-2 transfers sulfate to form MECA-79 epitope on various scaffold proteins, while GlcNAc6ST-1 favors MAdCAM-1 as a scaffold for GlcNAc-6-*O*-sulfation to form the MECA-79 epitope, suggesting scaffold protein-dependent sulfation by GlcNAc6ST-1.

GlcNAc6ST-1 Transfers Sulfate to Form the MECA-79 Epitope Preferentially on MAdCAM-1 but Only Marginally on CD34

To confirm the above findings, we established CHO cells stably expressing non-sulfated sialyl Lewis X attached to extended core 1 *O*-glycans (sialic acidα2→3Galβ1→4(Fucα1→3)GlcNAcβ1→3Galβ1→3GalNAcα1→Ser/Thr) (see Fig. 1) on either CD34 or MAdCAM-1, so that transfection of only a single GlcNAc6ST gene would form the MECA-79 epitope. As shown in Fig. 7, FACS analysis demonstrated that GlcNAc6ST-2 formed the MECA-79 epitope on both CD34 and MAdCAM-1, at almost the same level. GlcNAc6ST-1, on the other hand, formed only marginal levels of MECA-79 epitope on CD34, while it formed MECA-79 epitope on MAdCAM-1, although the efficiency was approximately 10 times lower than that of GlcNAc6ST-2.

We then carried out Western blotting to directly determine whether GlcNAc6ST-1 forms the MECA-79 epitope preferentially on MAdCAM-1 rather than CD34. As shown in Fig. 8, GlcNAc6ST-2 formed the MECA-79 epitope robustly on both CD34 and MAdCAM-1. On the other hand, as expected, GlcNAc6ST-1 formed the epitope exclusively on MAdCAM-1 although the band was very faint. These results combined indicate that GlcNAc6ST-1 transfers sulfate to form MECA-79 epitope preferentially on MAdCAM-1, but only marginally on CD34.

DISCUSSION

The present study demonstrates that decoration of MAdCAM-1 protein expressed on HEV-like vessels in colonic lamina propria with L-selectin ligand carbohydrates has potential clinicopathological significance in UC. We previously showed preferential induction of PNAd-expressing HEV-like vessels in the active phase of UC (14); however, in that study, we focused on CD34 as a scaffold protein for L-selectin ligand carbohydrates. Here, focusing on MAdCAM-1 as a scaffold protein, we delineate further the molecular mechanism involved in the pathogenesis of UC.

We showed that the proportion of MAdCAM-1^+ vessels in both active and remission phases of UC was significantly greater than that seen in normal colonic mucosa, while the proportion did not change significantly between the two phases, implying that the number of MAdCAM-1^+ vessels increases with an onset of active UC, but does not drop significantly with clinical remission. This result is supported by constitutive expression of MAdCAM-1 transcripts in UC, regardless of disease activity, as revealed by RT-PCR (see Fig. 5). We also showed that the percentage of MECA-79^+ vessels among MAdCAM-1^+ vessels in UC active phase was significantly greater than that seen in remission. Considering that L-selectin ligand carbohydrates co-localize with MAdCAM-1 protein at the luminal surface of HEV-like vessels, the above results suggest that UC disease activity is not directed by expression of MAdCAM-1 protein itself but rather by decoration of MAdCAM-1 protein with L-selectin ligand carbohydrates.

It is of interest what subsets of lymphocyte interact with decorated MAdCAM-1 expressed on HEV-like vessels induced in the colonic lamina propria with UC. Under physiological conditions, memory/effector lymphocytes (typically L-selectin^{low}, α4β7^{high}) but not naive lymphocytes (uniformly L-selectin^{high}, α4β7^{low}) are targeted to intestinal lamina propria (4,17). This can be explained by the fact that α4β7^{high} memory/effector lymphocytes effectively interact with MAdCAM-1-positive but L-selectin ligand-negative lamina propria venules via α4β7 integrin/MAdCAM-1 interaction for tethering and rolling and subsequent firm arrest, while α4β7^{low} naive lymphocytes are unable to initiate tethering and rolling on these venules (4,17). However, as shown here, with the onset of active UC, MAdCAM-1 expressed on intestinal lamina propria venules is decorated with L-selectin ligand

carbohydrates, as is observed in Peyer's patches and mesenteric lymph nodes, allowing participation of both L-selectin and α4β7 integrin in lymphocyte homing to intestinal lamina propria (4,17). Expression of both vascular addressins should support efficient binding to a fraction (approximately 20–25%) (34) of L-selectin-expressing memory/effector lymphocytes and even to naive lymphocytes (17).

A battery of glycosyltransferases and sulfotransferases has been shown to function in biosynthesis of L-selectin ligand carbohydrates, and as noted, GlcNAc6ST-1 (24) and GlcNAc6ST-2 (22) are likely required for sulfation of L-selectin ligand carbohydrates on HEVs (9). Under physiological states, the HEV-specific sulfotransferase GlcNAc6ST-2 has been shown to be more critical than GlcNAc6ST-1 in sulfating the C6-position of non-reducing GlcNAc on both extended core 1 and core 2 branched *O*-glycans on HEVs, particularly in peripheral lymph nodes (35); however, in our previous study, transcripts encoding GlcNAc6ST-2 were not detected in colonic mucosa with UC (14). Here, to confirm this finding, we performed nested PCR for GlcNAc6ST-2 and detected signals only in one sample from active phase UC and two from normal colonic mucosa; no remission phase samples were positive for GlcNAc6ST-2 mRNA. Nonetheless, our findings combined with those in the previous study (14) demonstrate preferential GlcNAc6ST-1 transcripts in the active phase of UC, suggesting that GlcNAc6ST-1 is likely the critical sulfotransferase regulating GlcNAc-6-*O*-sulfation of PNAd expressed on HEV-like vessels in UC.

We have shown here a scaffold protein-dependent property of GlcNAc6ST-1 for GlcNAc-6-*O*-sulfation as assessed by MECA-79 immunofluorescence staining (see Fig. 6 and 7). GlcNAc6ST-1 favors MAdCAM-1 as a substrate for GlcNAc-6-*O*-sulfation in MECA-79 epitope biosynthesis, a result consistent with our previous finding that GlcNAc6ST-1 is responsible for MECA-79 epitope biosynthesis in Peyer's patches, where MAdCAM-1 is preferentially expressed (35). On the other hand, GlcNAc6ST-2 apparently transfers sulfate to form MECA-79 epitope on any scaffold protein, including endogenous Lec2 cell membrane proteins. Thus, we hypothesize that GlcNAc6ST-1 decorates MAdCAM-1 protein with L-selectin ligand carbohydrates *in vivo*. Western blotting analysis demonstrates similar results, except for a very faint band corresponding to MAdCAM-1 sulfated by GlcNAc6ST-1 (see Fig. 8). This finding is consistent with our previous study in mice that GlcNAc6ST-2 efficiently transfers sulfate to extended core 1 *O*-glycans, generating substantial levels of MECA-79 epitope, while GlcNAc6ST-1 shows less efficient activity (35).

What determines scaffold protein-dependent preference of GlcNAc6ST-1 is unknown. Many factors influence the cellular substrate preferences of Golgi enzymes, such as Golgi distribution, association with other proteins, and intrinsic substrate binding activity (36). In the context of distribution, GlcNAc6ST-1 resides in the trans-Golgi network, whereas GlcNAc6ST-2 is more broadly distributed and more strongly represented in the earlier parts of the Golgi (37). Alternatively, underlying polypeptide sequence or secondary structure of MAdCAM-1 may contribute to a composite epitope preferentially recognized by GlcNAc6ST-1.

In conclusion, the present study demonstrates that decoration of MAdCAM-1 protein with L-selectin ligand carbohydrates is closely associated with UC disease activity. The findings are consistent with our hypothesis that lymphocytes are recruited to the colonic lamina propria with UC partly through L-selectin ligand carbohydrates attached to MAdCAM-1 and that such recruitment likely facilitates chronic inflammation and consequent clinical disease activity of UC. We also showed that GlcNAc6ST-1 shows a scaffold protein-dependent preference in GlcNAc-6-*O*-sulfation as assessed by MECA-79 epitope biosynthesis.

Whether only GlcNAc6ST-1 functions in biosynthesis of the L-selectin ligand carbohydrates on MAdCAM-1 protein *in vivo* awaits further studies.

Acknowledgments

Supported by the Ministry of Education, Culture, Sports, Science and Technology of Japan (Grants-in-Aid for Young Scientists B-18790240 and B-20790278 to M.K.), the Hokuto Foundation for Bioscience (Grant Award to M.K.), the Japan Society for the Promotion of Science (Grants-in-Aid for Scientific Research B-18390113 to J.N. and C-18590524 to J.M.), and the National Institutes of Health (Grants RO1 CA48737 and PO1 CA71932 to M.F.).

We thank Drs. Junya Mitoma, Hiroto Kawashima, Kenji Uchimura, and Tsutomu Nakada for helpful discussion, Mses. Kayo Suzuki and Matsuko Watanabe for technical assistance, and Dr. Elise Lamar for critical reading of the manuscript. Part of the work was presented as a poster at the annual meeting of the Society for Glycobiology, held in Boston, Massachusetts, during November 11–14, 2007.

References

1. Friedman, S.; Blumberg, RS. Inflammatory bowel disease. In: Braunwald, E.; Fauci, AS.; Kasper, DL., et al., editors. Harrison's Principles of Internal Medicine. 15. New York, NY: McGraw-Hill; 2001. p. 1679-1692.
2. Liu, C.; Crawford, JM. The gastrointestinal tract. In: Kumar, V.; Abbas, AK.; Fausto, N., editors. Robbins and Cotran Pathologic Basis of Disease. 7. Philadelphia, PA: Elsevier Saunders; 2005. p. 846-851.
3. Salmi M, Jalkanen S. Endothelial ligands and homing of mucosal leukocytes in extraintestinal manifestations of IBD. Inflamm Bowel Dis. 1998; 4:149–156. [PubMed: 9589300]
4. Butcher EC, Picker LJ. Lymphocyte homing and homeostasis. Science. 1996; 272:60–66. [PubMed: 8600538]
5. von Andrian UH, Mempel TR. Homing and cellular traffic in lymph nodes. Nat Rev Immunol. 2003; 3:867–878. [PubMed: 14668803]
6. Michie SA, Streeter PR, Bolt PA, et al. The human peripheral lymph node vascular addressin. An inducible endothelial antigen involved in lymphocyte homing. Am J Pathol. 1993; 143:1688–1698. [PubMed: 8256856]
7. Berlin C, Berg EL, Briskin MJ, et al. α4β7 integrin mediates lymphocyte binding to the mucosal vascular addressin MAdCAM-1. Cell. 1993; 74:185–195. [PubMed: 7687523]
8. Streeter PR, Rouse BT, Butcher EC. Immunohistologic and functional characterization of a vascular addressin involved in lymphocyte homing into peripheral lymph nodes. J Cell Biol. 1988; 107:1853–1862. [PubMed: 2460470]
9. Rosen SD. Ligand for L-selectin: homing, inflammation, and beyond. Annu Rev Immunol. 2004; 22:129–156. [PubMed: 15032576]
10. Yeh JC, Hiraoka N, Petryniak B, et al. Novel sulfated lymphocyte homing receptors and their control by a core 1 extension β1,3-*N*-acetylglucosaminyltransferase. Cell. 2001; 105:957–969. [PubMed: 11439191]
11. Aloisi F, Pujol-Borrell R. Lymphoid neogenesis in chronic inflammatory diseases. Nat Rev Immunol. 2006; 6:205–217. [PubMed: 16498451]
12. Renkonen J, Tynninen O, Hayry P, et al. Glycosylation might provide endothelial zip codes for organ-specific leukocyte traffic into inflammatory sites. Am J Pathol. 2002; 161:543–550. [PubMed: 12163379]
13. Kobayashi M, Mitoma J, Nakamura N, et al. Induction of peripheral lymph node addressin in human gastric mucosa infected by *Helicobacter pylori*. Proc Natl Acad Sci U S A. 2004; 101:17807–17812. [PubMed: 15591109]
14. Suzawa K, Kobayashi M, Sakai Y, et al. Preferential induction of peripheral lymph node addressin on high endothelial venule-like vessels in the active phase of ulcerative colitis. Am J Gastroenterol. 2007; 102:1499–1509. [PubMed: 17459027]

15. Briskin M, Winsor-Hines D, Shyjan A, et al. Human mucosal addressin cell adhesion molecule-1 is preferentially expressed in intestinal tract and associated lymphoid tissue. Am J Pathol. 1997; 151:97–110. [PubMed: 9212736]
16. Bargatze RF, Jutila MA, Butcher EC. Distinct roles of L-selectin and integrins α4β7 and LFA-1 in lymphocyte homing to Peyer's patch-HEV in situ: the multistep model confirmed and refined. Immunity. 1995; 3:99–108. [PubMed: 7542550]
17. Berlin C, Bargatze RF, Campbell JJ, et al. α4 integrins mediate lymphocyte attachment and rolling under physiologic flow. Cell. 1995; 80:413–422. [PubMed: 7532110]
18. Berg EL, McEvoy LM, Berlin C, et al. L-selectin-mediated lymphocyte rolling on MAdCAM-1. Nature. 1993; 366:695–698. [PubMed: 7505053]
19. Souza HS, Elia CC, Spencer J, et al. Expression of lymphocyte-endothelial receptor-ligand pairs, α4β7/MAdCAM-1 and OX40/OX40 ligand in the colon and jejunum of patients with inflammatory bowel disease. Gut. 1999; 45:856–863. [PubMed: 10562584]
20. Arihiro S, Ohtani H, Suzuki M, et al. Differential expression of mucosal addressin cell adhesion molecule-1 (MAdCAM-1) in ulcerative colitis and Crohn's disease. Pathol Int. 2002; 52:367–374. [PubMed: 12100519]
21. Imai Y, Lasky LA, Rosen SD. Sulphation requirement for GlyCAM-1, an endothelial ligand for L-selectin. Nature. 1993; 361:555–557. [PubMed: 7679207]
22. Hiraoka N, Petryniak B, Nakayama J, et al. A novel, high endothelial venule-specific sulfotransferase expresses 6-sulfo sialyl Lewis^{x}, an L-selectin ligand displayed by CD34. Immunity. 1999; 11:79–89. [PubMed: 10435581]
23. Fukuda M, Hiraoka N, Akama TO, et al. Carbohydrate-modifying sulfotransferases: structure, function, and pathophysiology. J Biol Chem. 2001; 276:47747–47750. [PubMed: 11585845]
24. Uchimura K, Muramatsu H, Kaname T, et al. Human *N*-acetylglucosamine-6-*O*-sulfotransferase involved in the biosynthesis of 6-sulfo sialyl Lewis X: molecular cloning, chromosomal mapping, and expression in various organs and tumor cells. J Biochem. 1998; 124:670–678. [PubMed: 9722682]
25. Uchimura K, Kadomatsu K, El-Fasakhany FM, et al. *N*-acetylglucosamine 6- *O*-sulfotransferase-1 regulates expression of L-selectin ligands and lymphocyte homing. J Biol Chem. 2004; 279:35001–35008. [PubMed: 15175329]
26. Shyjan AM, Bertagnolli M, Kenney CJ, et al. Human mucosal addressin cell adhesion molecule-1 (MAdCAM-1) demonstrates structural and functional similarities to the α4β7-integrin binding domains of murine MAdCAM-1, but extreme divergence of mucin-like sequences. J Immunol. 1996; 156:2851–2857. [PubMed: 8609404]
27. Schroeder KW, Tremaine WJ, Ilstrup DM. Coated oral 5-aminosalicylic acid therapy for mildly to moderately active ulcerative colitis. A randomized study. N Engl J Med. 1987; 317:1625–1629. [PubMed: 3317057]
28. Bibiloni R, Fedorak RN, Tannock GW, et al. VSL#3 probiotic-mixture induces remission in patients with active ulcerative colitis. Am J Gastroenterol. 2005; 100:1539–1546. [PubMed: 15984978]
29. Nakai K, Horton P. PSORT: a program for detecting sorting signals in proteins and predicting their subcellular localization. Trends Biochem Sci. 1999; 24:34–36. [PubMed: 10087920]
30. Aruffo A, Stamenkovic I, Melnick M, et al. CD44 is the principal cell surface receptor for hyaluronate. Cell. 1990; 61:1303–1313. [PubMed: 1694723]
31. Deutscher SL, Nuwayhid N, Stanley P, et al. Translocation across Golgi vesicle membranes: a CHO glycosylation mutant deficient in CMP-sialic acid transport. Cell. 1984; 39:295–299. [PubMed: 6498937]
32. Maly P, Thall A, Petryniak B, et al. The α(1,3)fucosyltransferase Fuc-TVII controls leukocyte trafficking through an essential role in L-, E-, and P-selectin ligand biosynthesis. Cell. 1996; 86:643–653. [PubMed: 8752218]
33. Duijvestijn AM, Horst E, Pals ST, et al. High endothelial differentiation in human lymphoid and inflammatory tissues defined by monoclonal antibody HECA-452. Am J Pathol. 1988; 130:147–155. [PubMed: 3276207]

34. Farstad IN, Halstensen TS, Kvale D, et al. Topographic distribution of homing receptors on B and T cells in human gut-associated lymphoid tissue: relation of L-selectin and integrin α4β7 to naive and memory phenotypes. Am J Pathol. 1997; 150:187–199. [PubMed: 9006335]

35. Kawashima H, Petryniak B, Hiraoka N, et al. *N*-acetylglucosamine-6-*O*-sulfotransferase 1 and 2 cooperatively control lymphocyte homing through L-selectin ligand biosynthesis in high endothelial venules. Nat Immunol. 2005; 6:1096–1104. [PubMed: 16227985]

36. de Graffenried CL, Bertozzi CR. The stem region of the sulfotransferase GlcNAc6ST-1 is a determinant of substrate specificity. J Biol Chem. 2004; 279:40035–40043. [PubMed: 15220337]

37. de Graffenried CL, Bertozzi CR. Golgi localization of carbohydrate sulfotransferases is a determinant of L-selectin ligand biosynthesis. J Biol Chem. 2003; 278:40282–40295. [PubMed: 12855678]

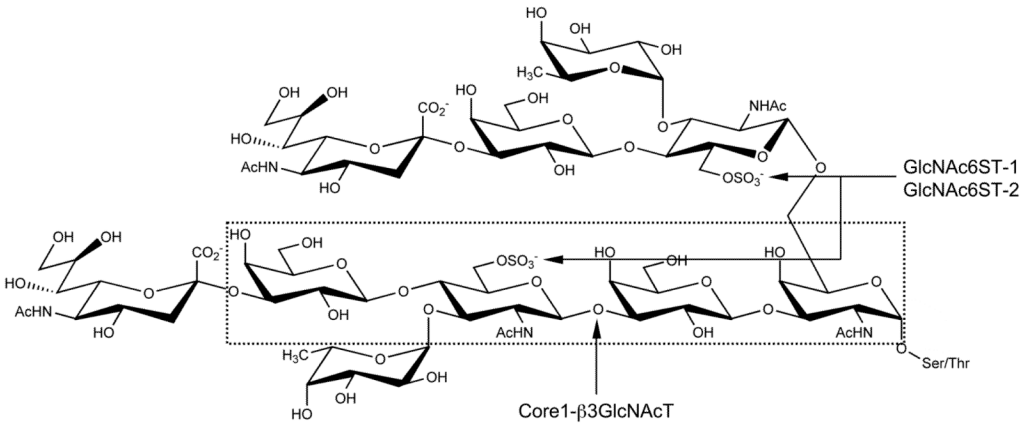

FIGURE 1.

Carbohydrate structure of L-selectin ligand. Core 1 *O*-glycans are extended by Core 1 extending β1,3-*N*-acetylglucosaminyltransferase (Core1-β3GlcNAcT) and sulfated by *N*-acetylglucosamine-6-*O*-sulfotransferase 1 (GlcNAc6ST-1) and/or GlcNAc6ST-2 to form 6-sulfo sialyl Lewis X attached to extended core 1 *O*-glycans. GlcNAc6ST-1 and/or GlcNAc6ST-2 also sulfate GlcNAc residue on core 2 branched *O*-glycans. 6-sulfo sialyl Lewis X attached to extended core 1 and/or core 2 branched *O*-glycans functions as an L-selectin ligand. The epitope for the MECA-79 monoclonal antibody (6-sulfo *N*-acetyllactosamine attached to extended core 1 *O*-glycans) is shown in dotted box.

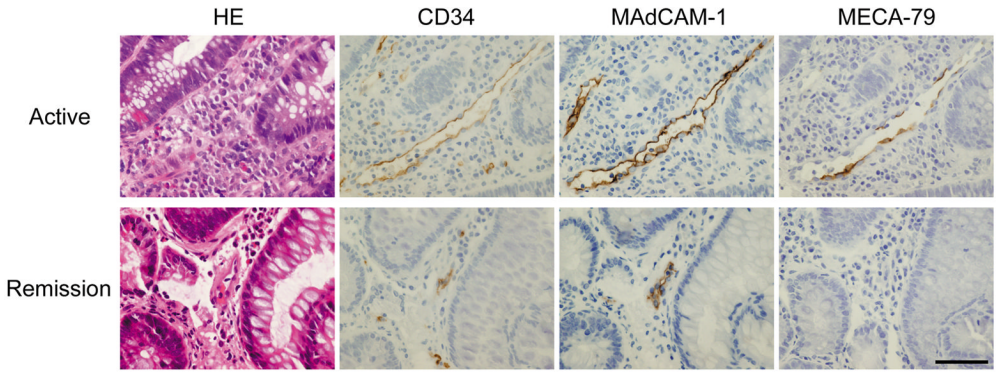

FIGURE 2.

Immunohistochemical profile of HEV-like vessels induced in UC. Serial tissue sections obtained from active (upper panels) and remission (lower panels) phases of UC were immunostained for CD34 (as a marker of vascular endothelial cells), MAdCAM-1, and PNAd (MECA-79). A fraction of $CD34^+$ vessels in the colonic lamina propria is also MAdCAM-1-positive, regardless of UC disease activity. In the active phase, $MAdCAM\text{-}1^+$ vessels are largely positive for MECA-79. HE = hematoxylin and eosin, Bar = 50 μm.

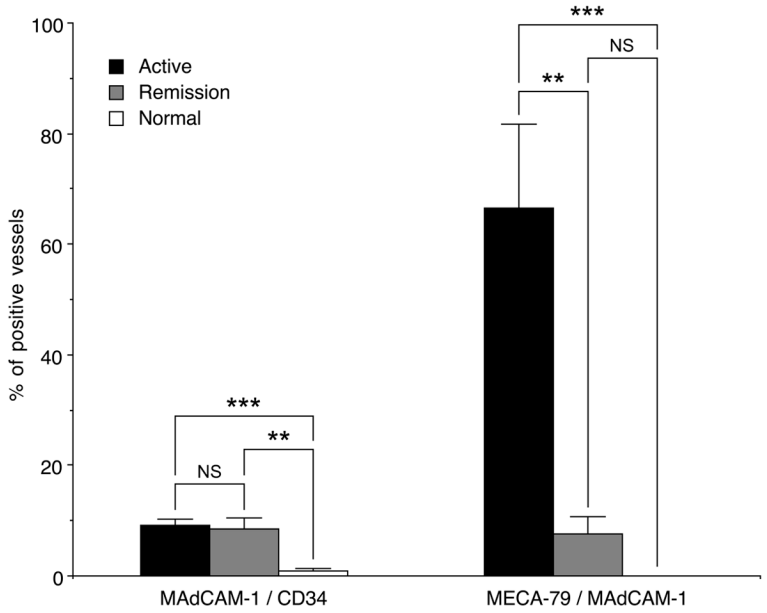

FIGURE 3.

Percentages of MAdCAM-1$^+$/CD34$^+$ and MECA-79$^+$/MAdCAM-1$^+$ vessels in active and remission phases of UC and normal colonic mucosa. The percentage of MAdCAM-1$^+$/CD34$^+$ vessels in UC in both phases is significantly greater than that seen in normal colonic mucosa, while percentages between the two phases do not differ significantly (left). The percentage of MECA-79$^+$/MAdCAM-1$^+$ vessels in active phase is significantly greater than those in remission phase and normal colonic mucosa (right). Data are presented as means (N = 32 in active phase, N = 12 in remission phase, and N = 10 in normal colonic mucosa) ± SEM. ** $P < 0.01$, *** $P < 0.001$, NS = not significant.

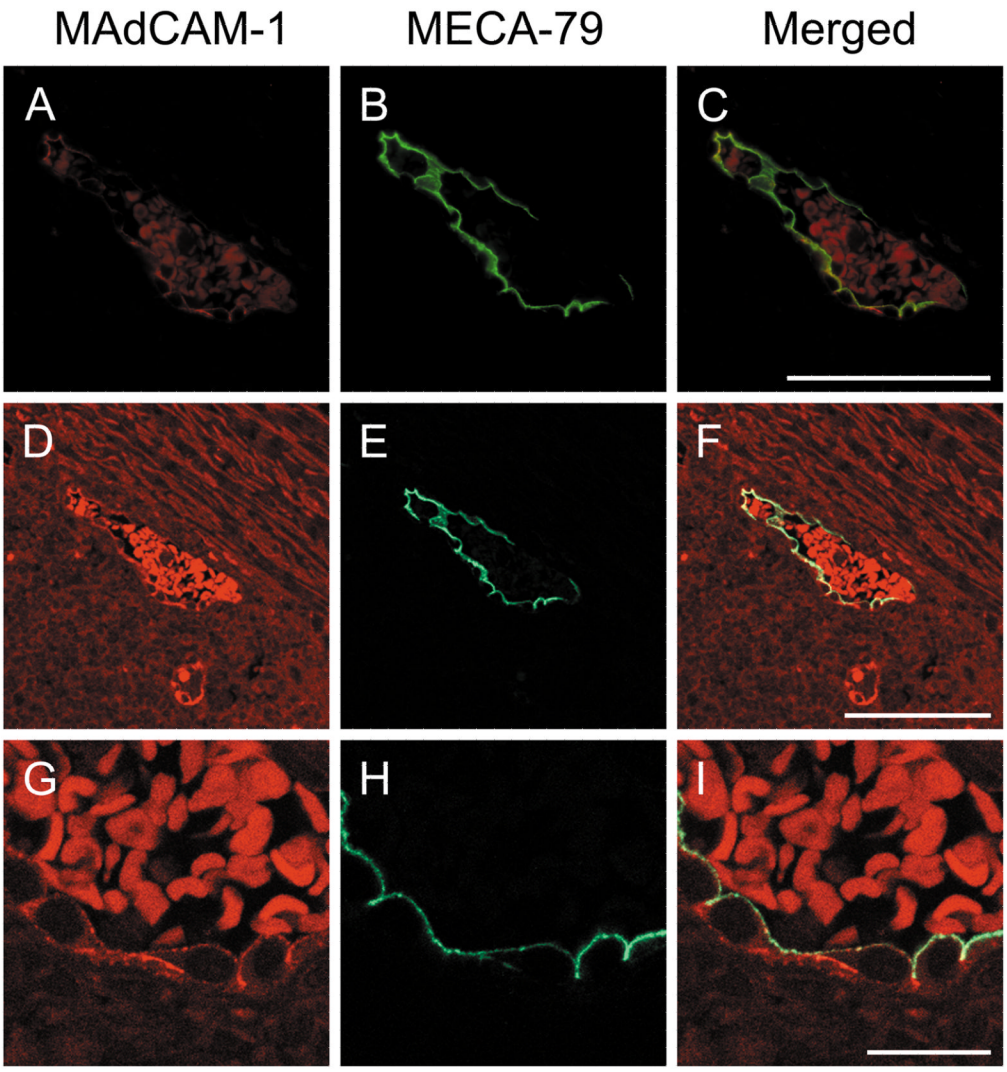

FIGURE 4.

Double immunofluorescence of HEV-like vessels in colonic lamina propria induced in active phase of UC. Tissue sections were doubly immunostained for MAdCAM-1 (red in A, D, G) and MECA-79 (green in B, E, H), and observed by a fluorescence microscope (A-C) and a laser confocal microscope (D-I). MECA-79^{+} L-selectin ligand carbohydrates co-localize with MAdCAM-1 at the luminal surface of HEV-like vessels, while MAdCAM-1 is expressed on almost the entire circumference of endothelial cells comprising HEV-like vessels. Co-localization is indicated as yellow in the merged image by yellow staining (C, F, I). Red signals within the vessel represent autofluorescence originating from red blood cells. Bar = 50 μm for A-F, and 10 μm for G-I.

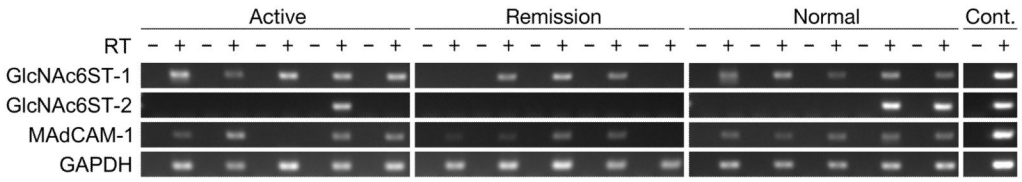

FIGURE 5.

Detection of MAdCAM-1 and GlcNAc6ST transcripts by RT-PCR. Total RNA was prepared from FFPE tissue sections with UC in active (N = 5) and remission (N = 5) phases along with normal colonic mucosa (N = 5). MAdCAM-1 is constitutively expressed in UC, regardless of disease activity (4/5 samples in both active and remission phases) as well as in normal colonic mucosa (5/5 samples). GlcNAc6ST-1 is transcribed in all patient samples of active UC and normal colonic mucosa, but in three of five samples with UC in remission phase. GlcNAc6ST-2 transcripts are detected in only one of five patient samples from UC in active phase and two of five normal colonic mucosa samples. Cont., control amplification using distilled water (-) and plasmid harboring the target cDNA (+).

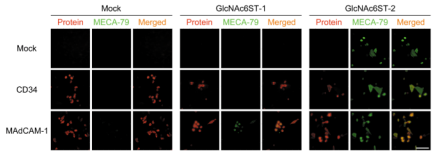

FIGURE 6.

Double immunofluorescence of Lec2 cells transiently transfected with either CD34, MAdCAM-1, or pcDNA1 (mock) vectors together with Core1-β3GlcNAcT cDNA and either GlcNAc6ST-1 (middle panels), GlcNAc6ST-2 (right panels), or pcDNA1 (mock) (left panels) vectors to detect core proteins (CD34 or MAdCAM-1) (red) and the MECA-79 epitope (green) simultaneously. GlcNAc6ST-2 (right panels) transfers sulfate to *N*-acetyllactosamine attached to extended core 1 *O*-glycans to form the MECA-79 epitope on all core proteins examined, including endogenous Lec2 cell membrane proteins, without apparent substrate preference for core protein. On the other hand, GlcNAc6ST-1 (middle panels) does not transfer sulfate to form the MECA-79 epitope on either CD34 or Lec2 membrane proteins, but does to MAdCAM-1. Bar = 50 μm.

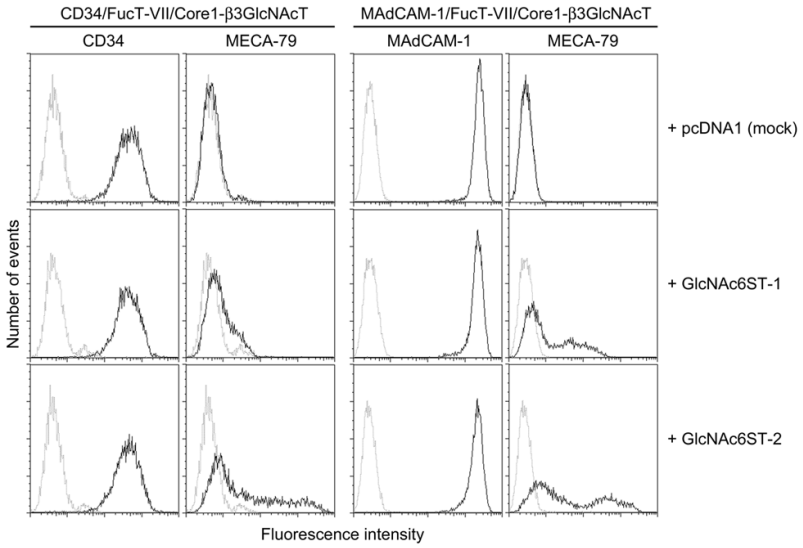

FIGURE 7.

FACS analysis of respective CHO-CD34/FucT-VII/Core1-β3GlcNAcT (left panels) and CHO-MAdCAM-1/FucT-VII/Core1-β3GlcNAcT (right panels) cells transiently transfected with either GlcNAc6ST-1 (middle panels), GlcNAc6ST-2 (lower panels), or pcDNA1 (mock) (upper panels) vectors. GlcNAc6ST-2 transfers sulfate to *N*-acetyllactosamine attached to extended core 1 *O*-glycans to form the MECA-79 epitope on both CD34 and MAdCAM-1 at similar levels (lower panels). On the other hand, GlcNAc6ST-1 transfers sulfate to form the MECA-79 epitope on MAdCAM-1 with approximately 1/10 efficiency of GlcNAc6ST-2; however, such an activity is marginal when MAdCAM-1 is substituted with CD34 (middle panels).

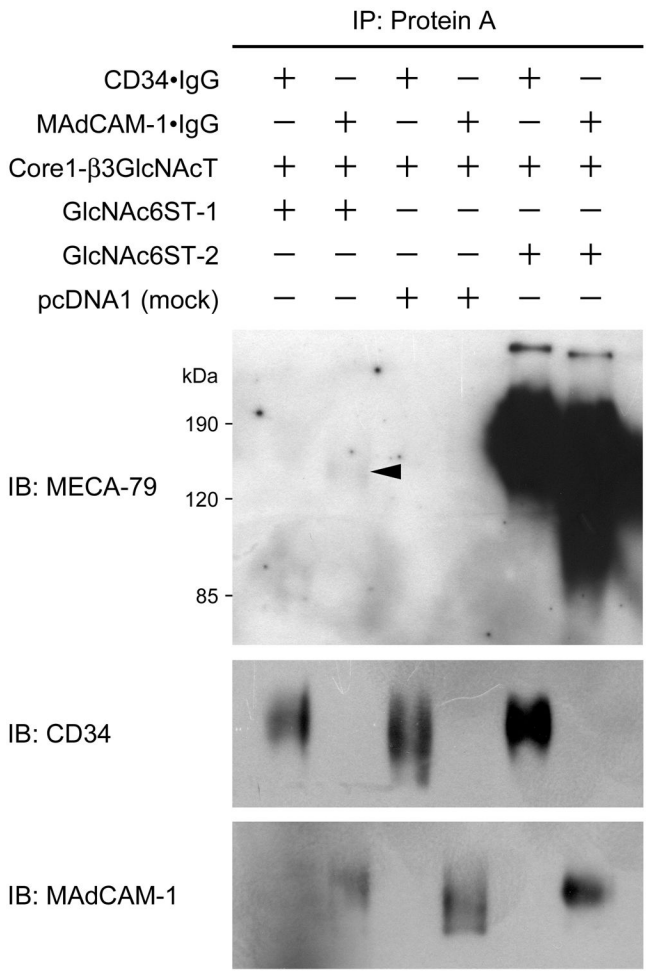

FIGURE 8.

Western blotting analysis of Protein A-Sepharose-purified glycoproteins CD34•IgG and MAdCAM-1•IgG obtained from the culture medium of Lec2 cells transiently transfected with either pcDNA1-CD34•IgG or pcDNA1-MAdCAM-1•IgG combined with pcDNA3-Core1-β3GlcNAcT and either pcDNA1-GlcNAc6ST-1, pcDNA1-GlcNAc6ST-2, or pcDNA1 (mock). GlcNAc6ST-2 robustly transfers sulfate to form the MECA-79 epitope on both scaffold proteins (CD34 and MAdCAM-1). On the other hand, GlcNAc6ST-1 very weakly but specifically forms MECA-79 epitope on MAdCAM-1 but not on CD34 (arrowhead).